PHYSICAL REVIEW E **82**, 035202(R) (2010)

Phase transitions in mixed populations composed of two types of self-oscillatory elements with different periods

Gouhei Tanaka,[1] Yusuke Okada,[2] and Kazuyuki Aihara[1,2]
[1]*Institute of Industrial Science, The University of Tokyo, Tokyo 153-8505, Japan*
[2]*Graduate School of Information Science and Technology, The University of Tokyo, Tokyo 113-8656, Japan*
(Received 6 May 2010; published 3 September 2010)

In globally coupled networks composed of oscillatory and nonoscillatory elements, the balance between the subpopulations plays an important role in network dynamics and phase transitions. To extend this framework, we investigate mixed populations consisting of two types of self-oscillatory elements with different periods, particularly given by limit cycle oscillators and period-doubled ones. Phase transitions in the mixed populations are elucidated by numerical bifurcation analyses of a reduced system. We numerically confirm a formula determining the critical balance between the subpopulations for a phase transition at sufficiently large coupling strength.

DOI: 10.1103/PhysRevE.82.035202 PACS number(s): 05.45.Xt, 02.30.Oz

Coupled nonlinear oscillators have been known to reproduce a rich variety of collective behavior like that observed in real-world systems [1,2]. In past several decades, a large number of theoretical and experimental studies on coupled oscillators have focused on synchronization phenomena [3]. Following early studies on coupled identical oscillators in regular networks, recently much attention has been paid to the introduction of additional realistic factors such as heterogeneity of couplings, complex network topologies, and stochastic noise.

Another possible practical assumption to be incorporated is individuality of constituent oscillators. Daido and Nakanishi [4,5] studied robustness of macroscopic synchronized oscillations in a globally coupled network of self-oscillatory (active) and non-self-oscillatory (inactive) elements linked by a Hopf bifurcation. This study was motivated by the problem of how an active behavior of coupled biological oscillators terminates as an increasing number of elements in the population alter their properties from active to inactive due to aging or disease. They found an *aging transition* which means that a global oscillation state turns into a quiescence state as the proportion of inactive elements exceeds a critical value for sufficiently large coupling strength. A universal property of the critical transition between oscillatory and quiescence regimes was revealed with a scaling law of an order parameter for network activity. A similar analysis was carried out for a mixed population of self-oscillatory and excitable elements linked by a saddle-node on invariant circle (SNIC) bifurcation [6].

Inspired by the above studies, we investigate a mixed population including two types of self-oscillatory elements with different periods. Our concern is not a transition between oscillatory and quiescence regimes but one between qualitatively different oscillatory regimes. Although such a system has been used as a model to reproduce a specific phenomenon such as biological rhythms generated by a mixed population of 20 h period and 24 h period circadian oscillators [7], phase transitions and universal properties have not yet been addressed. For simplicity, we focus on a special case where the two types of oscillators are linked by a period-doubling (PD) bifurcation. Namely, the period of one type of oscillator is almost twice as long as that of the other type. First, we investigate a mixed population of period-1 and period-2 limit cycle elements of the Rössler equation and elucidate its phase transitions through bifurcation analyses of a reduced system. Then, we discuss the universality of a formula for a critical balance between the two subpopulations at a period-doubling phase transition.

Following the previous studies [4–6], we assume that a population of a sufficiently large size N is divided into two groups, consisting of pN limit cycle elements (S_{L1}) and $(1-p)N$ period-doubled limit cycle elements (S_{L2}). The former and latter elements are called $L1$ and $L2$ elements, respectively. We consider a network with all-to-all diffusive coupling, where the state vector $\mathbf{x}_j$ of the jth element ($j=1,2,\ldots,N$) obeys the following equation:

$$\dot{\mathbf{x}}_j = \mathbf{F}_j(\mathbf{x}_j) + \frac{K}{N}\sum_{k=1}^{N}(\mathbf{x}_k - \mathbf{x}_j), \tag{1}$$

where $\mathbf{F}_j=\mathbf{F}_{L1}$ for $j \in S_{L1} \equiv \{1,2,\ldots,pN\}$ and $\mathbf{F}_j=\mathbf{F}_{L2}$ for $j \in S_{L2} \equiv \{pN+1,\ldots,N\}$.

First we investigate phase transitions in system (1) using the Rössler equation [8]: $\dot{x}=-y-z$, $\dot{y}=x+ay$, $\dot{z}=b+z(x-c)$. The Rössler equation with $a=b=0.2$ exhibits a typical period-doubling cascade as the control parameter c is varied. Figure 1 shows examples of period-1 and period-2 limit cycles in the Rössler equation to be coupled in the mixed population. The critical value of the first period-doubling bifurcation is given as $c^* \sim 2.832$. A globally coupled system of N Rössler units is described as follows:

$$\dot{x}_j = -y_j - z_j + \frac{K}{N}\sum_{k=1}^{N}(x_k - x_j), \tag{2}$$

$$\dot{y}_j = x_j + ay_j + \frac{K}{N}\sum_{k=1}^{N}(y_k - y_j), \tag{3}$$

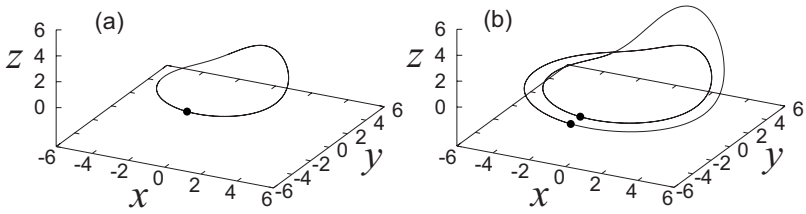

FIG. 1. Orbits of (a) a period-1 limit cycle at $c=2$ and (b) a period-2 limit cycle at $c=3$ in the single Rössler equation [8] with $a=b=0.2$.

$$\dot{z}_j = b + z_j(x_j - c_j) + \frac{K}{N}\sum_{k=1}^{N}(z_k - z_j), \tag{4}$$

where $\mathbf{x}_j=(x_j,y_j,z_j)$ is the state vector of the jth element for $j=1,\ldots,N$. The coupling strength is denoted by K. The parameters are set as follows: $a=b=0.2$, $c_j=c_{L1}=2$ for $j\in S_{L1}$, and $c_j=c_{L2}=3$ for $j\in S_{L2}$.

The network behavior of the coupled Rössler equations is dominated largely by two control parameters: the coupling strength K and the ratio p of $L1$ elements. Figure 2 shows the (K,p) phase diagram for a network with $N=100$, where different oscillatory regimes are distinguished by the brute-force method. In the regimes indicated by one-periodic and two-periodic oscillations, $L1$ and $L2$ elements are completely synchronized in each group, respectively, as shown in Figs. 3(a) and 3(b). For a sufficiently large value of K, the ratio p determines which of $L1$ and $L2$ elements entrains the others. In the remaining regime indicated by complex oscillations, the network exhibits more complex behavior including quasiperiodic and chaotic motions. Examples of quasiperiodic oscillations are shown in Figs. 3(c) and 3(d). Our purpose is to understand phase transitions in the (K,p) diagram of the globally coupled system.

In the regimes where $L1$ and $L2$ elements are perfectly synchronized in each group respectively, system (1) can be essentially reduced to the following two-element system:

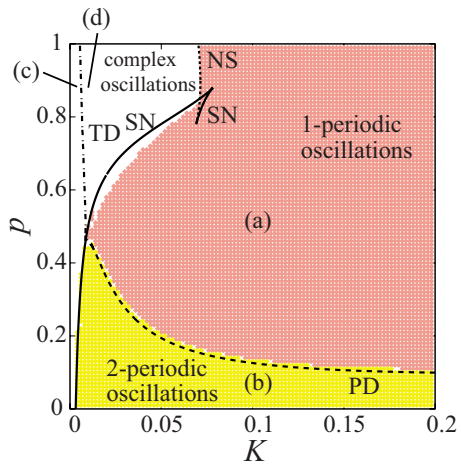

FIG. 2. (Color online) The (K,p) phase diagram for $N=100$ populations composed of period-1 and period-2 limit cycle elements of the Rössler equation. The parameter space is separated into three regions corresponding to one-periodic, two-periodic, and more complex oscillations, respectively. The superimposed curves indicate bifurcation sets of the reduced system, including SN, PD, NS, and TD bifurcations. Attractors at the parameter values indicated by (a)–(d) are shown in Fig. 3.

$$\dot{\mathbf{x}}_{L2} = \mathbf{F}_{L2}(\mathbf{x}_{L2}) + Kp(\mathbf{x}_{L1} - \mathbf{x}_{L2}), \tag{5}$$

$$\dot{\mathbf{x}}_{L1} = \mathbf{F}_{L1}(\mathbf{x}_{L1}) + K(1-p)(\mathbf{x}_{L2} - \mathbf{x}_{L1}), \tag{6}$$

where $\mathbf{x}_j=(x_j,y_j,z_j)$ for Rössler units $(j=L1,L2)$. This reduction enables us to treat p as a continuous parameter in the limit of $N\to\infty$. To locate bifurcation points of a periodic solution in the reduced system, a Poincaré map P is constructed with a cross section $x_{L2}=0$. A local bifurcation point is obtained by simultaneously solving the fixed point condi-

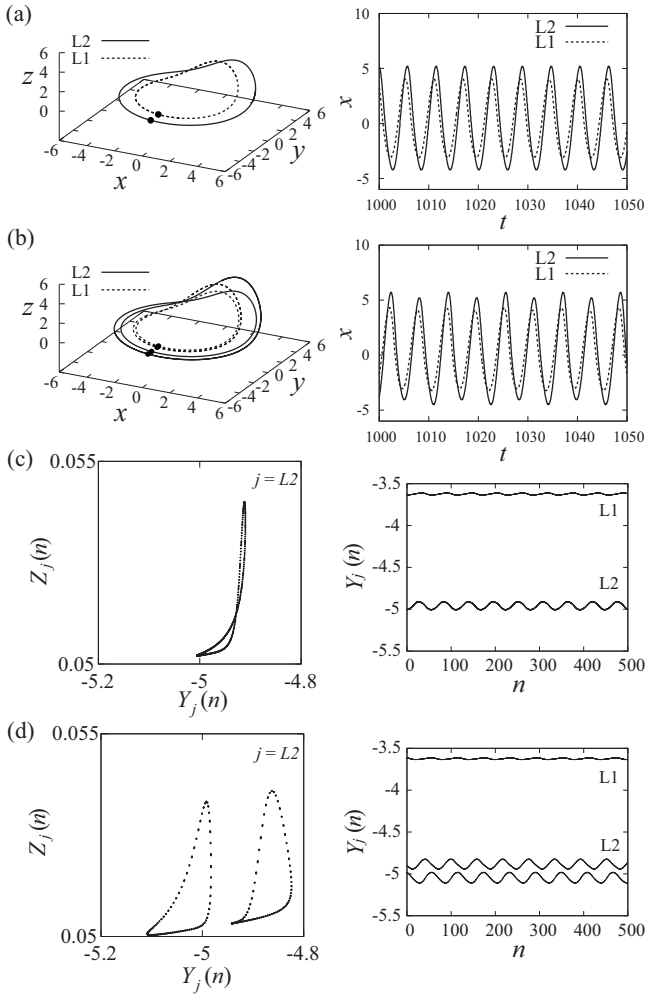

FIG. 3. Phase portraits (left) and time series (right). (a) One-periodic oscillations at $(K,p)=(0.1,0.5)$. (b) Two-periodic oscillations at $(K,p)=(0.1,0.1)$. (c) Quasiperiodic oscillations at $(K,p)=(0.006,0.9)$. $(Y_j(n),Z_j(n))$ denotes the nth component in a sequence of discrete points $(y_j(t),z_j(t))$ at the moment when $x_j(t)=0$. (d) Quasiperiodic oscillations (doubled torus) at $(K,p)=(0.007,0.9)$.

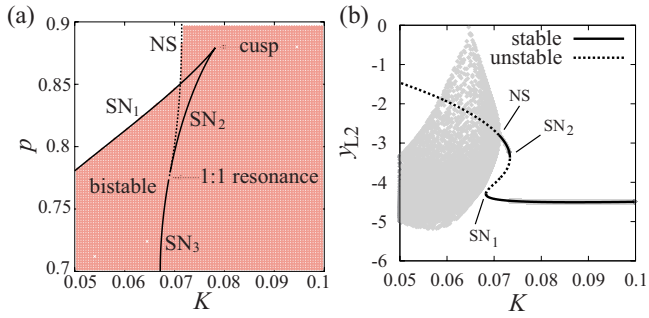

FIG. 4. (Color online) Bistability in the reduced system. (a) The (K,p) phase diagram around the nonsmooth boundary point between the regular and complex regimes. (b) The one-parameter bifurcation diagram along the horizontal arrow in (a) where p is fixed at 0.84. The branch of fixed points of the Poincaré map corresponds to a limit cycle, which leads to a quasiperiodic solution via a Neimark-Sacker bifurcation.

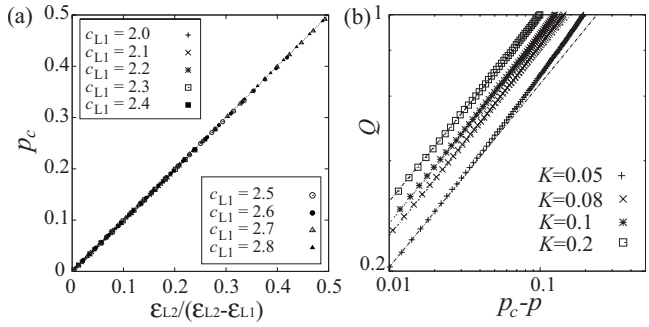

FIG. 5. (a) The critical value p_c between the one-periodic and two-periodic regimes, numerically evaluated at $K=50$. Formula (7) holds for various combinations of c_{L1} and c_{L2} values. For each c_{L1} value in the inset, the cases with many different c_{L2} values are indicated by the same mark. (b) Critical scaling of the normalized order parameter $Q=M(p)/M(0)$ near $p=p_c$ in the log-log plot. The slope of the line fitting the plots for each K value is 0.5.

tion $P(w)-w=0$ and the characteristic equation $\chi(\mu)=\det(\mu I-\partial P/\partial w)=0$, where w is a fixed point of the Poincaré map, I is the unit matrix, and the multiplier μ specifies the bifurcation type, i.e., $\mu_1=1$ for saddle-node (SN), $\mu_1=-1$ for PD, and $\mu_{1,2}=e^{\pm i\theta}$ with $\theta\neq 0,\pi$ for Neimark-Sacker (NS) bifurcations [9]. The torus doubling (TD) bifurcation is located by a heuristic method as described later. As shown in Fig. 2, the phase transitions in the globally coupled system are well understood by the bifurcation curves of the reduced system, although some differences between them arise due to the finiteness of the population and a destabilization of the clustering state with two synchronized groups in system (1).

The saddle-node and Neimark-Sacker bifurcation curves in Fig. 2 account for the transition between the regular oscillation regime and the complex one. The Neimark-Sacker bifurcation found at values of p close to 1 explains the birth of a quasiperiodic attractor corresponding to a two-dimensional torus. The nonsmoothness of the phase transition boundary is caused by the intersection between the Neimark-Sacker and saddle-node bifurcation curves. Figure 4(a) shows an enlarged phase diagram around the nonsmooth boundary point in the reduced system. There are two saddle-node bifurcation curves connected at the cusp point, between which two attractors coexist. Such bistability is also observed in the globally coupled system. The saddle-node and Neimark-Sacker bifurcation curves collide at the codimension-2 bifurcation point called 1:1 resonance characterized by a fixed point of P with multipliers $\mu_1=\mu_2=1$ [10]. Figure 4(b) shows a one-parameter bifurcation diagram along the horizontal arrow in Fig. 4(a). The curve corresponds to a one-periodic limit cycle. In the bistability region, a stable limit cycle (lower branch) coexists with the other one (upper branch) or a quasiperiodic attractor. However, it should be noted that the bistability region is not necessarily present in the (K,p) phase diagram for different combinations of c_{L1} and c_{L2} values because the bifurcation curves can be scaled and the nonsmooth boundary point can be moved outside the parameter space with $p<1$.

In the complex oscillation regime, we observe a quasiperiodic solution corresponding to a sequence of discrete points forming an invariant closed curve (ICC) on the section $x_j=0$ as shown in Fig. 3(c). In Fig. 3(d), on the other hand, the discrete points form two ICCs alternately. The transition from a quasiperiodic solution with one ICC to that with two ICCs is called torus doubling [11]. Since the $L1$ and $L2$ elements are nearly synchronized in each group, respectively, the bifurcation set of torus doubling can also be understood by the reduced system. For a quasiperiodic solution, we obtain time sequences of discrete points on the section: $\mathbf{X}_j=(y_j,z_j)$ with $x_j=0$ and $\dot{x}_j>0$ for $j=L_1,L_2$. We calculate the centroid $\mathbf{X}_c(m)$ of the sequence with sampling period m and evaluate the error $|\mathbf{X}_c(1)-\mathbf{X}_c(2)|$. The error should be zero for a torus with one ICC, while positive for a doubled torus with two ICCs. Therefore, as shown in Fig. 2, we can specify the torus doubling point using a sufficiently small threshold value $(=10^{-6})$ for the error.

Now we discuss a universal property of the phase transition in system (1). As shown in Fig. 2, the boundary between the one-periodic and two-periodic oscillation regimes in the globally coupled Rössler system can be understood as a period-doubling bifurcation of a reduced system in the limit of $N\to\infty$. As K increases, the critical value p_c of the period-doubling bifurcation seems to converge to a certain value. The critical p value for period doubling in the limit of $K\to\infty$ can be written as follows:

$$p_c^{\infty}=\frac{\epsilon_{L2}}{\epsilon_{L2}-\epsilon_{L1}}, \tag{7}$$

where $\epsilon_{L2}=c^*-c_{L2}<0$ and $\epsilon_{L1}=c^*-c_{L1}>0$ with $c^*\sim 2.832\,434\,793\,231$. This is supported by the numerical result in Fig. 5(a). For various possible combinations of c_{L1} and c_{L2} values, the numerically obtained critical value p_c for a sufficiently large value of K is in good agreement with the left-hand side of Eq. (7). Equation (7) shows that the critical proportion of $L1$ and $L2$ elements for the phase transition is determined by the parameters in the individual elements. Surprisingly this result is consistent with the previous studies with oscillatory and nonoscillatory elements [4,6]. The generality of Eq. (7), which was analytically derived for Hopf

and SNIC bifurcation cases [6], is enhanced by our numerical verification in the period-doubling transition case. This is one of the main results of this Rapid Communication.

We can characterize the period-doubling transition using the order parameter defined as $M=\langle|\overline{\mathbf{X}_j-\langle\mathbf{X}_j\rangle}|\rangle$ for discrete-time sequences of $\mathbf{X}_j=(y_j,z_j)$ with $x_j=0$ and $\dot{x}_j>0$, where $\langle\cdot\rangle$ means a long-term average and the overbar means an ensemble average. As shown in Fig. 5(b), the normalized order parameter $Q=M(p)/M(0)$ is well fitted by the line with a slope of 1/2 near $p=p_c$ in the log-log scale, i.e., $M\propto(p_c-p)^{1/2}$. Similar power-law scaling was analytically obtained for the other transitions [4,6].

We expect that formula (7) holds for a general mixed population composed of period-2^m and period-2^{m+1} self-oscillatory elements linked by a period-doubling bifurcation ($m=0,1,\ldots$). Additionally, such a population can exhibit complex oscillations which are brought about by interactions between two types of limit cycle oscillators when the coupling strength K is small. Figure 6(a) shows a phase diagram for a mixed population composed of period-2 and period-4 limit cycle elements of the Rössler equation. Its structure is rather similar to that shown in Fig. 2. Figure 6(b) shows a phase diagram for a mixed ensemble of period-1 and period-2 limit cycle elements of the Hindmarsh-Rose neuron model [12]: $\dot{x}_j=y_j-ax_j^3+bx_j^2+I-z_j$, $\dot{y}_j=c-dx_j^2-y_j$, $\dot{z}_j=r_j(S(x_j-x_1)-z_j)$, with parameter values $a=1$, $b=3$, $c=1$, $d=5$, $S=4$, $x_1=-1.6$, $I=3.47$ [13], $r_j=r_{L1}=0.002$ for $j\in S_{L1}$, and $r_j=r_{L2}=0.006$ for $j\in S_{L2}$. Although the mechanism of a transition from regular to more complex oscillation regimes is different from the Rössler model case, the phase transition between one-periodic and two-periodic oscillation regimes is similar to Fig. 2. We have numerically confirmed that formula (7) is also valid for these two cases [14].

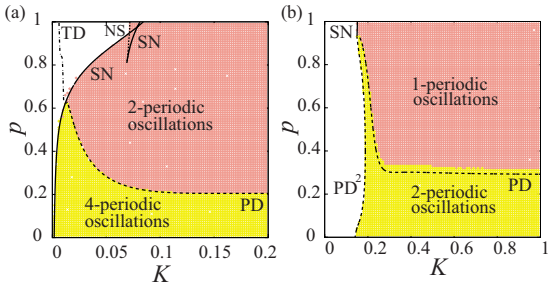

FIG. 6. (Color online) Phase diagrams in mixed populations with $N=100$ of (a) period-2 ($c_{L1}=3.0$) and period-4 ($c_{L2}=4.1$) limit cycle elements of Rössler equation and (b) period-1 and period-2 limit cycle elements of the Hindmarsh-Rose neuron model.

In summary, we have investigated phase transitions in mixed populations composed of two types of self-oscillatory elements with different periods, especially using limit cycle elements and period-doubled ones. Numerical bifurcation analyses of the reduced model have well explained the phase transitions in the globally coupled populations. We have numerically confirmed the formula for the critical balance between the two subpopulations at the phase transition and obtained numerical results suggesting its universality. This study can be a useful step to understand the effect of individuality of elements in a network and establish a method to control network dynamics by adjusting the balance of the numbers of subpopulations.

The authors thank Dr. H. Daido for his valuable comments. This work was partially supported by JSPS through "Funding Program for World-Leading Innovative R&D on Science and Technology (FIRST Program)."

[1] Y. Kuramoto, *Chemical Oscillations, Waves, and Turbulence* (Springer-Verlag, Berlin, 1984).
[2] A. T. Winfree, *The Geometry of Biological Time*, 2nd ed. (Springer, New York, 2001).
[3] A. Pikovsky, M. Rosenblum, and J. Kurths, *Synchronization—A Universal Concept in Nonlinear Sciences* (Cambridge University Press, Cambridge, England, 2001).
[4] H. Daido and K. Nakanishi, Phys. Rev. Lett. **93**, 104101 (2004).
[5] H. Daido and K. Nakanishi, Phys. Rev. E **75**, 056206 (2007).
[6] D. Pazó and E. Montbrió, Phys. Rev. E **73**, 055202(R) (2006).
[7] S. Bernard, D. Gonze, B. Čajavec, H. Herzel, and A. Kramer, PLOS Comput. Biol. **3**, e68 (2007).
[8] O. E. Rössler, Phys. Lett. **57A**, 397 (1976).
[9] H. Kawakami, IEEE Trans. Circuits Syst. **CAS-31**, 246 (1984).
[10] Y. A. Kuznetsov, *Elements of Applied Bifurcation Theory*, Applied Mathematical Sciences Vol. 112 (Springer, New York, 1995).
[11] H. Kaneko, Prog. Theor. Phys. **69**, 1806 (1983).
[12] J. L. Hindmarsh and R. M. Rose, Proc. R. Soc. London, Ser. B **221**, 87 (1984).
[13] Y. S. Fan and A. V. Holden, Chaos, Solitons Fractals **3**, 439 (1993).
[14] See supplementary material at http://link.aps.org/supplemental/10.1103/PhysRevE.82.035202 for figures supporting formula (7).